

UC San Diego

UC San Diego Electronic Theses and Dissertations

Title

Soft Robot Actuation Strategies for Locomotion in Granular Substrates

Permalink

<https://escholarship.org/uc/item/6m29n5gk>

Author

Ortiz, Daniel Hernandez

Publication Date

2018

Peer reviewed|Thesis/dissertation

UNIVERSITY OF CALIFORNIA SAN DIEGO

Soft Robot Actuation Strategies for Locomotion in Granular Substrates

A Thesis submitted in partial satisfaction of the requirements for the degree Master of

Science

in

Engineering Sciences (Mechanical Engineering)

by

Daniel Hernandez Ortiz

Committee in charge:

Professor Michael Tolley, Chair
Professor Mauricio de Oliveira
Professor Nicholas Gravish

2018

Copyright

Daniel Hernandez Ortiz, 2018

All rights reserved

The Thesis of Daniel Hernandez Ortiz as it is listed on UC San Diego Academic Records is approved, and it is acceptable in quality and form for publication on microfilm and electronically:

Chair

University of California San Diego

2018

DEDICATION

This Thesis is dedicated to all the people that made it possible. I would also like to dedicate this to my family for their constant support without which none of this would have been possible. Lastly, I would like to dedicate this to my girlfriend Phuong Tran for her constant support and positive energy, which inspired me to keep going on the days I couldn't. Thank you all very much for the love and encouragement.

TABLE OF CONTENTS

Signature Page.....	iii
Dedication.....	iv
Table of Contents.....	v
List of Figures.....	vii
Acknowledgments.....	ix
Abstract of the Thesis.....	x
Chapter 1 Introduction.....	1
1.1 Background.....	1
1.2 Annelid Inspiration.....	4
1.3 Summary.....	6
Chapter 2 Methods.....	8
2.1 Experimental Design.....	8
2.2 Robot Design, Fabrication, and Actuation.....	10
2.3 Granular Substrates Enclosure.....	15
2.4 Constant Force Single-Segment Experiments.....	15
2.5 Constant Velocity Single-Segment Experiments.....	17
2.6 Tethered Three-Segment Digging.....	18
Chapter 3 Results.....	21
3.1 Constant Force Single-Segment Experiments.....	21
3.2 Constant Velocity Single-Segment Experiments.....	23
3.3 Tethered Three-Segment Digging.....	26
Chapter 4 Discussion.....	28

Chapter 5 Conclusion.....	30
References.....	31

LIST OF FIGURES

Figure 1: Bioinspired actuation for a soft robot capable of digging in granular media....4	
Figure1 A: Bioinspired soft robot capable of digging in granular substrates4	
Figure1 B: Bioinspired actuation strategies for a soft-robot capable of digging.....5	
Figure 2: Experimental setup used for constant velocity and force experiments.....9	
Figure 3: Plot of initial experiment to determine the frequency of the robot actuation....12	
Figure 4: Plot of the initial experiment to determine appropriate pressure for actuation..13	
Figure 5: Diagram and images of constant velocity setup.....14	
Figure 6: Diagram and model of constant force setup.....16	
Figure 7: Diagram and image of unassisted tube and granular setup.....18	
Figure 8: Diagram and images of peristaltic cycle.....20	
Figure 9: Results of constant force experiments.....22	
Figure 9 A: Constant force experiment with 4.5 N applied.....22	
Figure 9 B: Constant force experiment with 6 N applied.....22	
Figure 9 C: Constant force experiment with 7.5 N applied.....22	
Figure 9 D: Constant force experiment with 9 N applied.....22	
Figure 9 E: Summary of constant force experiment.....23	
Figure 10: Results of constant velocity experiments.....24	
Figure10 A: Constant velocity experiment at 0.5 mm/sec.....24	
Figure10 B: Constant velocity experiment at 1.0 mm/sec.....24	
Figure10 C: Constant velocity experiment at 2.0 mm/sec.....25	

Figure 10 D: Summary of constant velocity experiments.....	25
Figure 11: Results of the granular and tube experiments.....	26

ACKNOWLEDGEMENTS

I would like to acknowledge Professor Michael Tolley for his support and as the chair of my committee. He has been an invaluable resource and his guidance has been greatly appreciated throughout this process. I would also like to acknowledge Professor Nicholas Gravish for his support and expertise in the subject matter of granular materials. None of this would have been possible without these two professors and their dedication to research. I would like to acknowledge Professor Michael Tolley and Professor Nicholas Gravish for coauthoring this thesis in full, which has been submitted for publication as it may appear in IEEE Xplore, 2019, Ortiz, Daniel; Gravish, Nick; and Tolley, Michael T. The thesis author was the primary investigator and author of this material.

ABSTRACT OF THE THESIS

Soft Robot Actuation Strategies for Locomotion in Granular Substrates

by

Daniel Hernandez Ortiz

Master of Science in Engineering Sciences (Mechanical Engineering)

University of California San Diego, 2018

Professor Michael T. Tolley, Chair

Soft bodied organisms such as *annelids* may exploit body compliance by using their hydrostatic skeletons and muscles to burrow in granular substrates. The prevalence and performance of soft structures in biology has inspired researchers to incorporate soft materials into new robotic systems with adaptive and robust qualities. In this work, we investigate the design of soft digging robots inspired by the bristled worm, (*polychaetas*).

The behavior of soft structures in granular environments is complex and still not well understood. We detail the experiments, design, and fabrication of a soft robotic

system capable of maneuvering in granular substrates and investigate actuation strategies for drag reduction inspired by the bristled worm's biomechanical behaviors. The soft robotic system is composed of three main actuator segments, with the leading segment being the focus of interest for analysis of this complex locomotion. We implemented and studied two methods of actuation in our soft-robot: peristaltic expansion and bi-directional bending.

We compared the drag force experienced by the leading segments that reproduce these active strategies to the force experience by rigid, and unactuated, soft versions. We find that biomechanical behaviors can have a significant impact on locomotion strategies in granular substrates. Based on these results, we demonstrate a tethered, three-segment soft robot capable of digging through granular media. In summary, we find that over a range of movement speeds, soft-robots performing peristaltic expansion at their tip experience the least drag force. Soft-robots with unactuated tips experienced the largest drag resistance emphasizing the importance of controlling the tip stiffness to enable effective subsurface movement

Chapter 1

Introduction

This chapter defines the background and motivation for the scope of this thesis as well as introduces some key concepts for soft robotic actuation strategies inspired by annelids. Besides this it also discusses the biomechanical behaviors that inspired these actuation strategies followed by a summary of each chapter.

1.1 Background

Granular substrates (GS) are collections of solid particles. Examples of natural GS range from snow and sand to a variety of soils. These materials have many unusual qualities that allow them to behave as a fluid, solid, and gas, depending on the loading conditions. When an external perturbation is applied, these materials can transition between these states and generate complex reaction forces. Conventional, rigid robotic systems typically perform well on hard, flat surfaces, yet movement across granular substrates can be challenging and may require special wheels or a continuous track to maneuver.

The forces associated with locomotion in granular materials relies on an understanding of the inhomogeneous stress distribution in the bulk of the media. This inhomogeneous stress distribution is due to the anisotropic and irregular formation of resistive force chains [1]. To create motion in granular material a localized force must reorganize the resistive grains in its path, which changes the packing distributions along the path of motion. The packing distribution of the material is an important factor in determining the flow and force dynamics [2]. The irregular nature of these resistive pockets gives the applied force a stick slip quality. As the packing density increases so does the force fluctuations.

In addition to movement across granular substrates, movement within these substrates may be advantageous for applications such as construction, environmental monitoring, and surveillance. Given the limitations of rigid robots, we propose a soft robot inspired by biology for solving the problem of maneuvering in and on this complex material. The study of granular substrates and flowing particle interaction is comprehensive [1]–[12]; however, there are limited studies for how compliant systems interact in these dynamic materials [13], [14]. This chapter discusses our inspiration for solving this problem as well as limitations to current approaches.

Scientists and engineers have turned to animals and the principles surrounding their locomotion to solve many problems of robot mobility in a wide range of environments [15]–[19]. In the context of locomotion on and within granular substrates, this bioinspired approach has proven successful in producing novel robot designs, gaits,

and control methods. For example, the sidewinder rattlesnake (*Crotalus cerastes*) inspired a robot capable of traversing sloped GS [20], the razor clam (*E. directus*) inspired a system capable of burrowing by fluidization [21], and the sandfish lizard (*S. Scincus*) inspired another system for swimming through GS [22]. There are also strategies for legged locomotion and for walking on deformable substrates inspired by a variety of lizards and crabs [23]–[25].

Although the previous examples solve the problem of moving in and on GS with rigid robots, most animals are not completely rigid and are instead composed of tissues that exhibit a range of stiffnesses, e.g. skin, muscles, fat, cartilage, bones, and tendons. The resulting compliance of their bodies allows animals to conform to complex shapes in various terrains, and to absorb impacts when in motion. Recently, scientists have incorporated compliance in a novel soft robot design that is capable of tip extension and granular fluidization to maneuver in granular materials [13]. Incorporating soft materials into robotic systems may provide many advantages for solving the problem of maneuvering on and in GS including enhanced durability of the system, ability to conform the robot's body to surroundings, and robust actuation in these unstructured environments [16], [26]–[28].

Top View

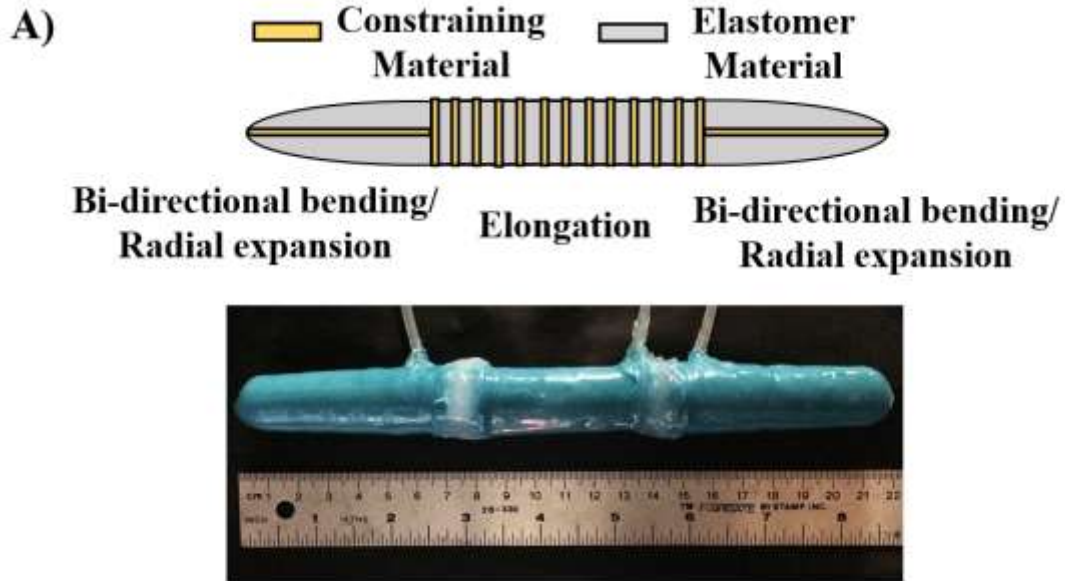


Figure 1 A: Bioinspired soft-robot capable of digging in granular substrates. Schematic and image of the soft robotic system dyed green for visualization in clear granular material.

1.2 Annelid Inspiration

For this study, we take inspiration from *Polychaetas*, a class of marine annelids that live and burrow in granular environments. *Polychaetas* exhibit a range of behaviors during locomotion including bi-directional bending or side-to-side head movement to remove material from its path, peristaltic expansion motion to anchor their position

while elongating forward and expanding the cavity through crack propagation, and rapid eversion of a proboscis to quickly expand the burrowing cavity [29]–[31].

Side View

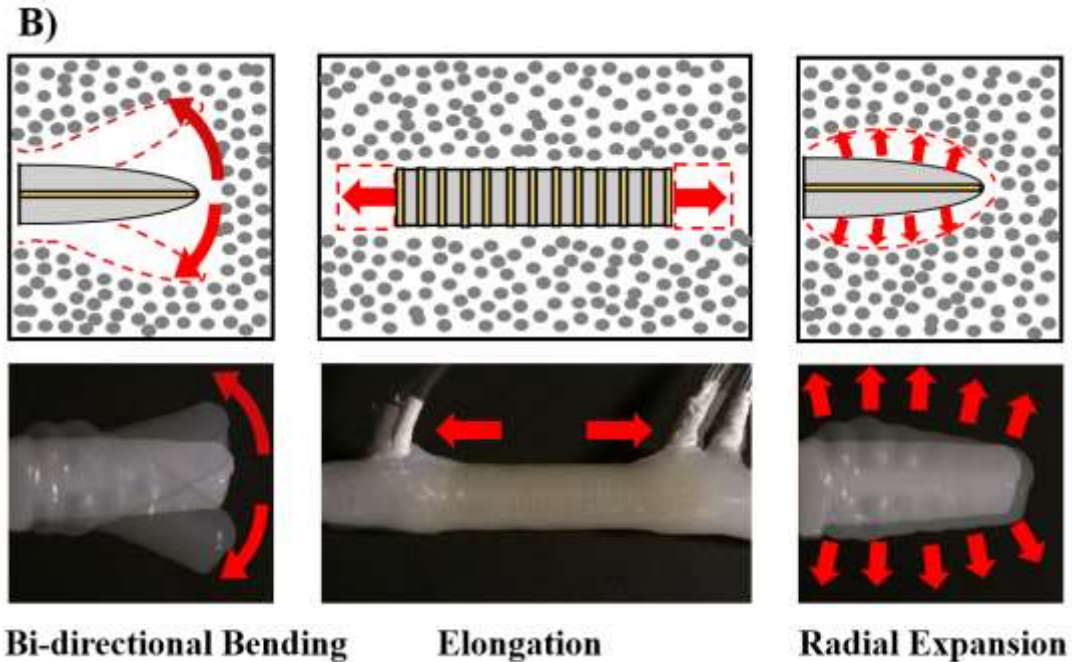


Figure 1 B: Bioinspired actuation strategies for a soft-robot capable of digging in granular substrates. Schematic and image of biomechanical behaviors (bi-directional bending and radial expansion) and elongation.

Polychaetas (*Nereis diversicolor*) are capable of burrowing in underwater granular substrates to depths reaching a maximum of approximately 29 cm. The burrowing depth depends on food supply and predation risk [32]. Understanding these mechanisms may provide insight into locomotion in GS and aid in understanding the

forces being exerted on soft deformable bodies. Peristaltic motion and bi-directional bending are the most amenable to replication in a soft robotic system (Fig. 1B). This study has the potential to help with various applications such as construction, pipe inspection, exploration of hazardous environments e.g. avalanches and earthquakes, and subsurface exploration on other planets.

Peristaltic motion is generated by volumetric expansion and contraction of radial and longitudinal muscles in retrograde waves. This wave of muscular contractions allows annelids to apply normal force on the burrow walls, and thus anchor their position in unstructured terrain while elongating forward [33]. Previous work has used soft robotic systems inspired by earthworms to replicate peristaltic motion [34], [35]. Although numerous attempts have been made to replicate this biomechanical behavior through various techniques [34]–[39], no attempts have been made in demonstrating and examining the drag forces in unstructured granular environments. Much of the previous work has examined the biomechanical behaviors in structured environments such as piping, vents, and along relatively smooth surfaces.

1.2 Summary

This paper presents experimental validation that *Polychaeta* inspired behaviors and compliant materials can be implemented in robotic applications for drag reduction and locomotion in granular environments. The remainder of this paper discusses the experimental design decisions, the physical soft robotic system, the fabrication, and

experimental methods in Section II. We describe the results in Section III, discuss the findings in Section IV, and provide concluding remarks in Section V.

Chapter 2

Methods

This chapter discusses the methods and techniques used to explore actuation strategies for locomotion in granular substrates. Specifically, this chapter goes into detail about the experiments used to examine the drag forces associated with locomoting in these complex materials. In addition, it also discusses the soft robot design, fabrication, and actuation.

2.1 Experimental Design

The first parameters we investigated were the frequency and pressure of the pneumatic actuation required to optimize the amplitude of the bending and extension of the soft segments of the robot. Next, we performed experiments in a granular environment where a constant force was applied to all the soft-robot segment configurations while collecting position data along our enclosure. We also performed experiments where the velocity of locomotion was held constant and the resistive force was measured as the soft segment was dragged through the granular media along the length of the experimental enclosure. Lastly, we submerged a tethered version of the entire soft robotic worm in the

granular media and tracked its position during unassisted locomotion. To compare this last experiment against an ideal case of unassisted locomotion, we also ran an experiment in an acrylic tube and visually recorded its change in position.

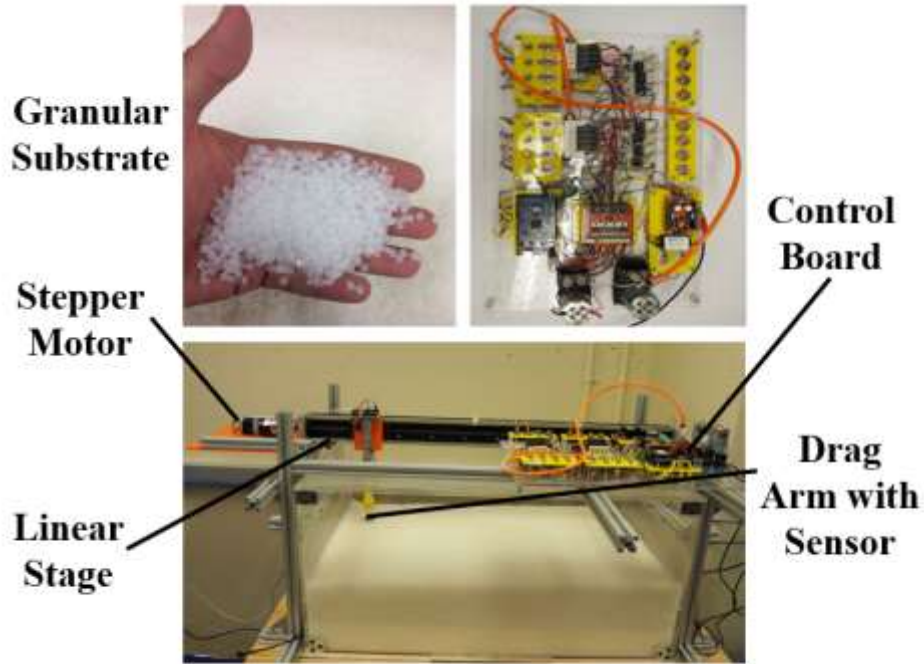


Figure 2: Experimental enclosure used for constant velocity experiments and control system for actuating the soft-robot. Images of the experimental enclosure (bottom), the polypropylene pellets (top-left), pneumatic control system (top-right).

All our experiments took place in a custom acrylic granular enclosure (Fig. 2). For the experiments where force and velocity were held constant, we chose four soft robot tip configurations to focus on: periodic radial expansion/ peristaltic motion, bi-directional

bending, an unactuated soft intruder, and an unactuated rigid intruder. These robot tip configurations helped us determine differences to consider for maneuvering in GS. Each of these experiments focused on the leading segment of our soft robotic system except the unassisted experiments, which used the entire three segment soft-robot and was used to examine the locomotion strategy with the least amount of drag.

2.2 Robot Design, Fabrication, and Actuation

The soft robotic system we used in this study consists of three silicone pneumatic actuators in series. We selected three actuators because it is the minimum requirement to generate peristaltic motion, although in theory more segments can be added to increase the size of the robot. We chose a platinum cured silicone elastomer (Dragon Skin 10, Smooth-On) for the actuators because of its low stiffness (Shore value of 10A). This silicone elastomer has amorphous characteristics which allow it to elongate up to a maximum of 663% [40]. These material properties allow us to inflate the robotic actuators at relatively low pressures with a minimum actuation pressure of 55 kPa for our design (Fig.1A).

Soft actuators can be mechanically programmed to expand, twist, bend, and elongate by varying the orientation of the constraining material and the geometry [41]. To generate the desired bending motion for our soft robotic system, we designed a series of pneumatic networks or Pneu-nets which utilized a thinner geometry between the channels [42]. To generate bending in two directions we included a strain limiting layer

between two sets of Pneu-nets. To constrain the radial expansion of elongation segments, we wrapped polyaramid thread around the circumference of a hollow elastomeric tube (Fig. 1A).

We delivered pressurized air separately to each of these segments through silicone tubes. For a robot capable of both bi-directional bending at the leading segment and peristaltic motion a minimum of four pneumatic lines are needed. We connected the tubing to the soft robot perpendicular to the plane of motion for simplicity and to help us visually track its movement with red markers when it was submerged in the GS.

To fabricate the soft robot, we first designed the negative of each actuator in CAD software. From this 3D model we then 3D printed a mold of the negative. We then cast actuator halves in these molds from two-part silicone elastomer (Dragon Skin 10, Smooth-On Inc.) with a 1:1 mixture ratio. After curing two halves, we bonded them to a central constraining layer with a silicone adhesive, which created two independent chambers for the leading actuator. To make an elongating motion in the middle actuator, we applied the constraining layer to the outside by manually wrapping polyaramid thread around the radius.

After assembling the segments, we coated them with two more layers of silicone by painting the layers on manually to add more thickness to the outer wall and seal the constraining materials. These added layers of silicone material allowed the actuator to withstand higher pressures up to a maximum of 124 kPa. To fully assemble a robotic system, we bonded an alternating pattern of expanding/bending segments followed by

elongating segments with nonwoven polyester/cellulose cloth between each to seal each segment independently (Fig. 1A). After we bonded the soft robot together, we punched holes in the top of each independent segment and attached pneumatic lines using the silicone adhesive.

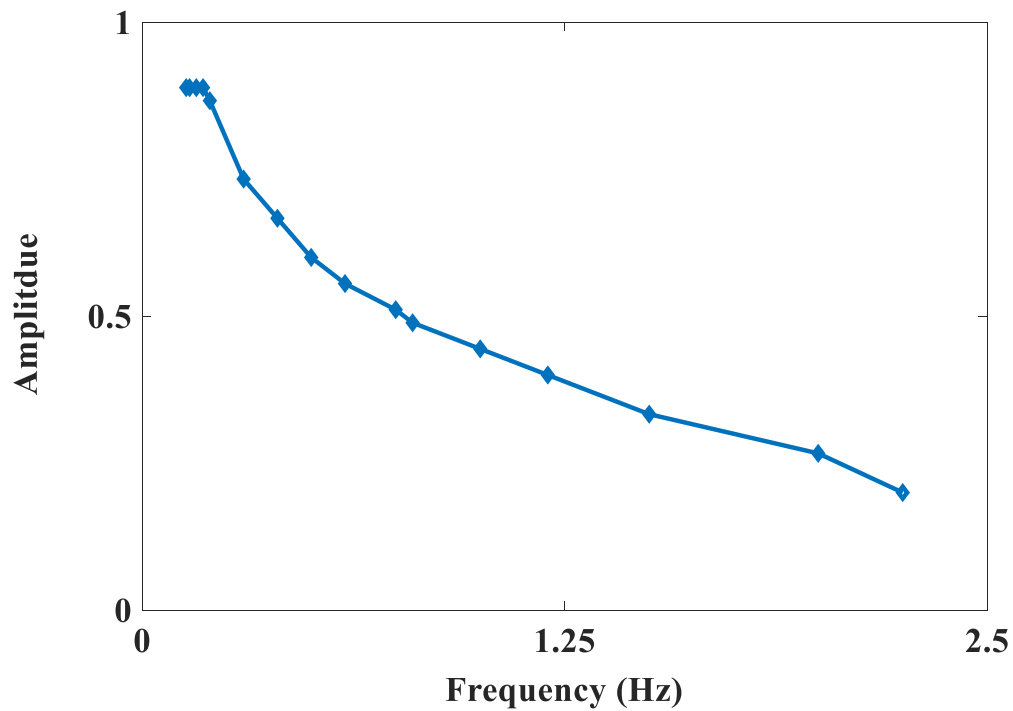


Figure 3: Plot of the initial experiment to determine the frequency of the soft robot actuation normalized by the maximum bending distance (4cm). The amplitude of bending was obtained by inflating the leading robot segment at a constant pressure of 96 kPa for a given valve frequency.

To control the actuation of the soft components for all the experiments we used an open-source fluidic control board [43] (Fig. 2). The first task was to determine the frequency of actuation for the bi-directional and radial actuators. Through experimentation, we determined that a frequency of approximately 0.4 Hz maintained approximately 80% of the bending amplitude with the maximum amplitude being approximately 4 cm (Fig.3). Coincidentally, biological annelids have roughly the same stride frequency [44].

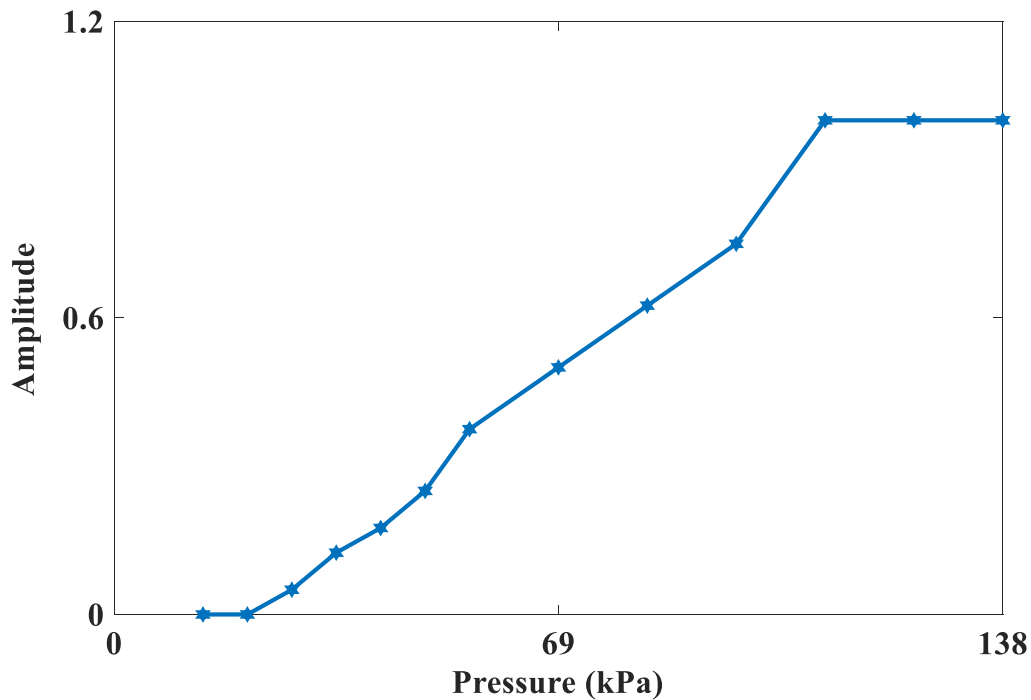


Figure 4: Plot of the initial experiment to determine the pressure of the soft robot actuation, where the amplitude of bending was normalized by the maximum bending distance (4cm). The maximum pressure which lead to fail after a few cycles was 138 kPa.

We found that a constant pressure of approximately 96 kPa achieved 80% of the bending amplitude, and that the maximum bending occurred near failure at 110 kPa (Fig 4). To isolate the leading segment for the constant force and velocity experiments, we attached a silicone plate slightly larger than the thickest diameter of the robot and press-fit the intruder into a rigid bracket. The rigid bracket made the actuator mountable to our experimental setup (Fig. 5).

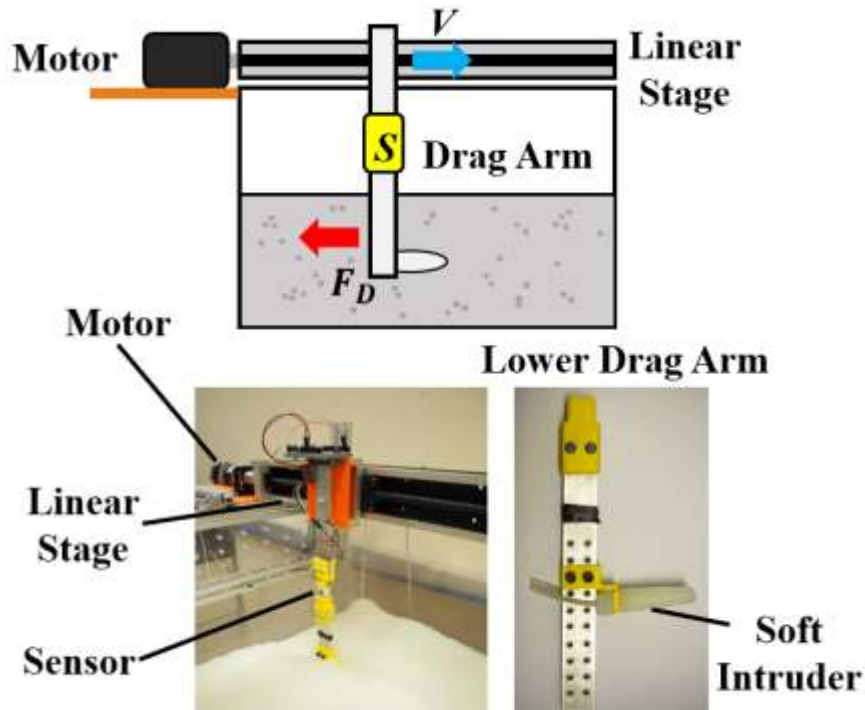


Figure 5: Diagram (top) and images (bottom) of constant velocity experiment to measure the drag forces experienced by various digging soft-robot segment configurations.

2.3 Granular Substrate Enclosure

We performed all the experiments for this work in an acrylic enclosure filled with plastic polypropylene pellets, (Fig.2). These particles were chosen because of their heterogeneous shape, and most importantly because this material has a volume fraction of 0.5 similar to a sand silt mixture [45]. The volume fraction for the polypropylene pellets was calculated as $\phi = V_p/V$ where ϕ denotes the volume fraction, V_p the volume of the particles, and V the total volume. The volume fraction plays a very important role in the dynamics of GS in response to stress [46]. We chose a depth of 5 cm for all the assisted experiments because it was the lowest depth at which movement was visible at the surface.

2.4 Constant Force Single-Segment Experiments

To measure and examine the steady-state velocity of our segment in GS, when applying a constant force, we performed an experiment using an incremental rotary encoder with 600 pulses per revolution (PPR) resolution. This rotary encoder was attached to a pulley which we connected to a linear slide with an aluminum arm (Fig. 6). Initially, we qualitatively determined the range of applied forces to use by performing some basic experiments: For these initial experiments we incrementally loaded the system with the minimal mass required to overcome the resistive force of the material and initiate

movement for each of the four configurations (no actuation both rigid and soft, radial expansion, and bi-directional bending). Based on these tests, we determined the constant forces for this experiment to be 4.5N, 6 N, 7.5 N, and 9 N. We also chose to use an experiment length of approximately 300 mm located near the center of the enclosure to avoid any effects due to the boundaries.

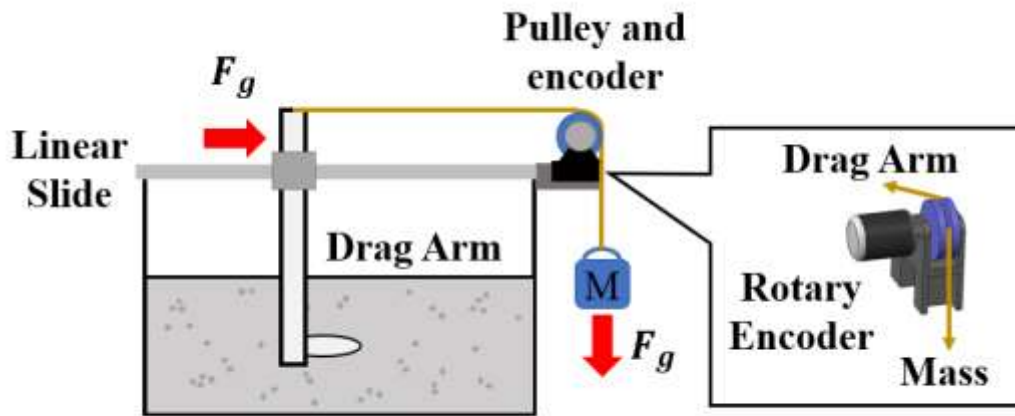


Figure 6: Diagram of constant force experimental setup (left) and model of the pulley and encoder (right) used to measure velocity of the drag arm using a rotary encoder to collect position data.

The first set of tests involved the mass pulley system where a constant force was applied until it traveled 300 mm or fell below the threshold velocity of 0.01 mm/sec. The experiments all started with the soft intruder being held mechanically at rest until the actuation was initiated at which point it was released. After this initial release the system was run until either the intruder became stuck and fell below the velocity threshold or

until it moved the full distance of the experiment. If the system reached the full distance of 300 mm, we stopped the experiment. We ran this experiment three times for each method of actuation for each of the four constant forces. The particle bed was raked and mixed before each new trial to ensure the removal of any compactions in the material due to settling.

2.5 Constant Velocity Single-Segment Experiments

To measure the drag force occurring at a constant velocity, we used a linear stage with an attached aluminum arm and embedded a load cell capable of measuring up to 98 N of force with a 0.01 N resolution (Fig. 5). The linear stage was driven using a 15:1 geared stepper motor (NEMA 23, Dongyang Dongzhueng Motor Co.) capable of generating enough torque to overcome the resistive force of the granular material. We ran the experiment at constant velocities of 0.5 mm/sec, 1 mm/sec, and 2 mm/sec. The embedded load cell measured the deflection of the arm to calculate the resistive force impeding motion. We chose these speeds based on the speeds measured during the constant force experiments. We measured the drag force for the same four configurations of the leading segment: 1) bi-directional bending, 2) periodic radial expansion, 3) soft and unactuated, and 4) rigid unactuated.

The constant velocity experiments started with the leading intruder being actuated immediately followed by the linear stage being driven by the stepper motor. We performed this experimental sequence to ensure the soft intruder would not start off being

forced to the side of least resistance and influence the measured deflection of the aluminum arm. We then continued the experiment over a 300 mm distance, after which we shut off the robot segment actuation and stepper motor. The experiments were performed a total of three times for each method of actuation for all three constant velocities. The granular bed was raked and thoroughly mixed prior to each of the trials.

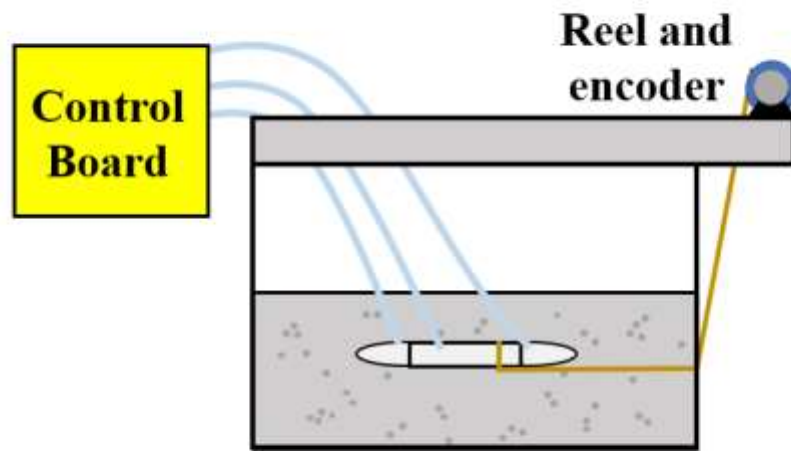


Figure 7: Diagram of the unassisted granular experiment using the three-segment tethered soft-robot.

2.6 Tethered Three-Segment Digging

To verify the tethered soft robot could maneuver without assistance and to examine the best performing behavior to reduce the drag force, we ran an experiment

using peristaltic actuation to generate self-propelled motion (Fig. 8). For these experiments, we submerged the soft robot up to red markers we placed on the pneumatic lines in the center of the tank away from the walls to minimize any effects due to the boundaries (Fig. 7). We attached a string to the soft robot and the other end was spooled around a reel with a mounted encoder.

As the soft robot moved forward, the unspooling string rotated the pulley, providing the displacement of the robot. We ran this experiment until the velocity of the robot decreased below a threshold of 0.01 mm/s. As before, we raked the particles prior to each experiment.

As a point of comparison, we also tested the system in an acrylic pipe to get a comparison of the ideal performance scenario in a structured environment (Fig. 11). For this scenario, we ran a total of three trials and visually recorded its progress through the acrylic tube. This experiment used the same actuation frequency and as the granular experiments.

Peristaltic Cycle

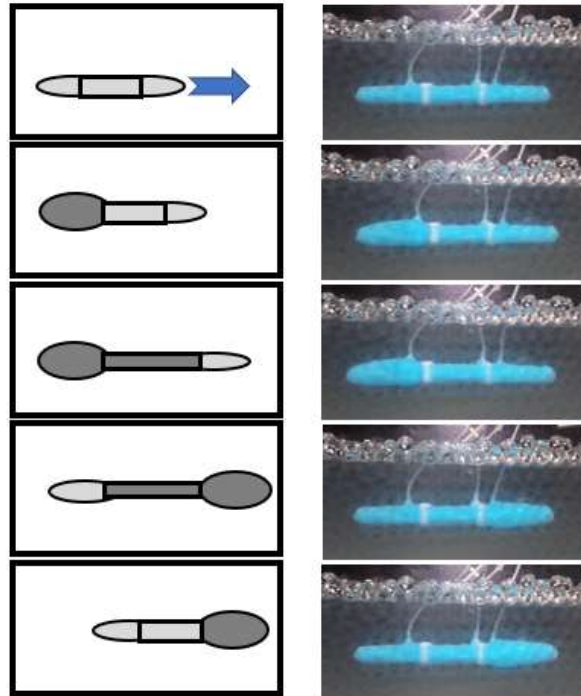


Figure 8: Diagram of the peristaltic cycle used for the tethered three-segment experiments. (Left) is a diagram of the peristaltic cycle used to show how locomotion is created, (Right) Images of the peristaltic cycle in clear hydrogel beads for visualization purposes.

Chapter 3

Results

This chapter discusses the results obtained from the three experiments: constant force to a single-segment, constant locomotion velocity of a single-segment, and Tethered three-segment digging experiments. Specifically, this chapter goes into detail about the steady-state velocity, drag force, and distance traveled.

3.1 Constant Force Single-Segment Experiments

The results of the constant force experiments can be seen in Fig. 9. The periodic radial expansion achieved the highest steady-state velocity for all the cases. The radial expansion configuration was also able to move the entire 300 mm distance without getting stuck, for all cases of constant force. The soft robot segment configuration that was able to achieve the second highest steady-state velocity for all cases of constant force was bi-directional bending. Both robot segments with no actuation (rigid and soft) got stuck in the granular material or fell below the threshold of 0.01mm/sec for every level of applied force. Of the unactuated robot segments, the soft unactuated segment moved the least (Fig. 9E).

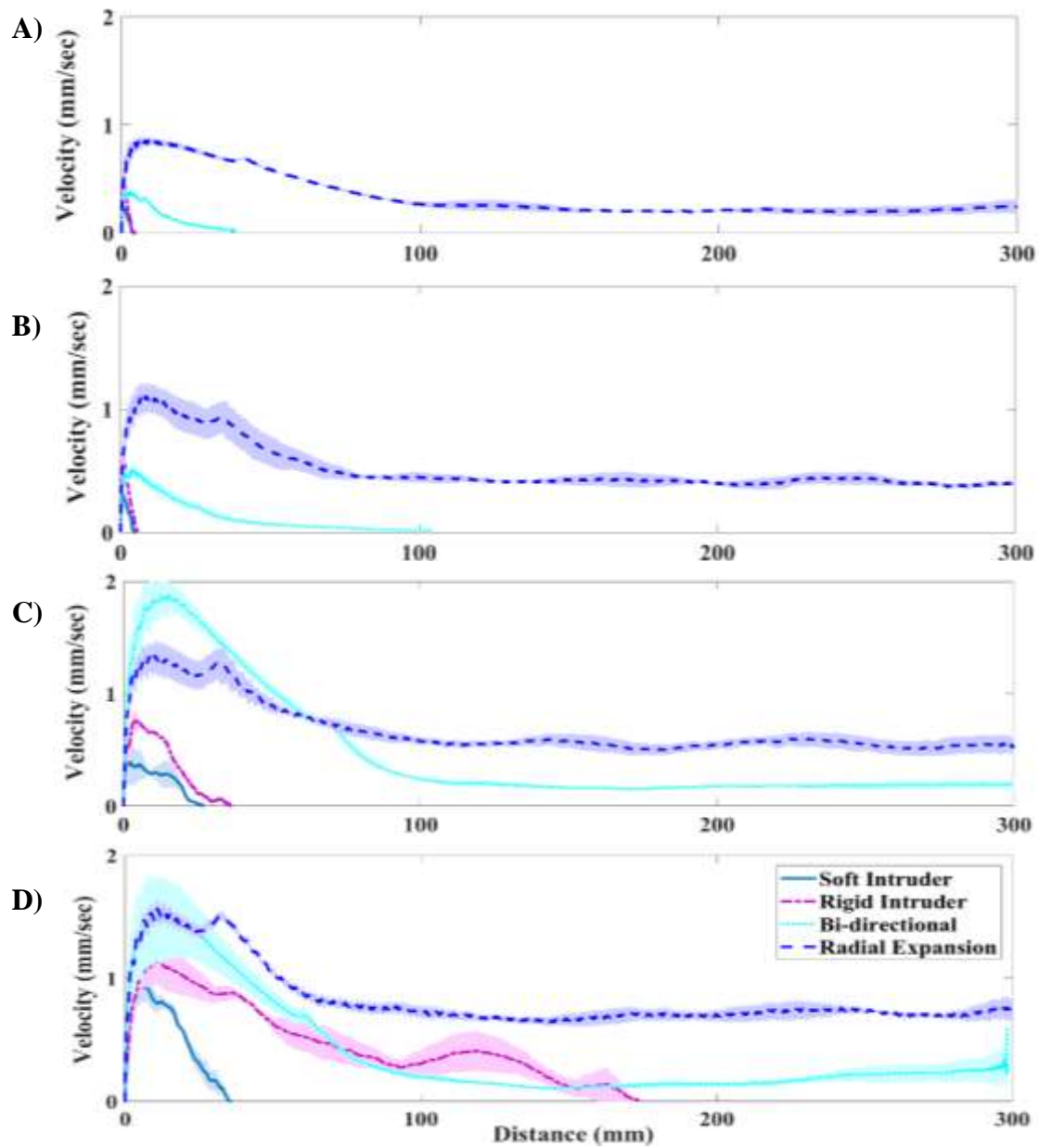


Figure 9 A-D: Results of constant force experiments where position data was collected using a rotary encoder. (A)-(D) Raw data for four applied forces 4.5 N (A), 6 N (B), 7.5 N (C), and 9 N (D).

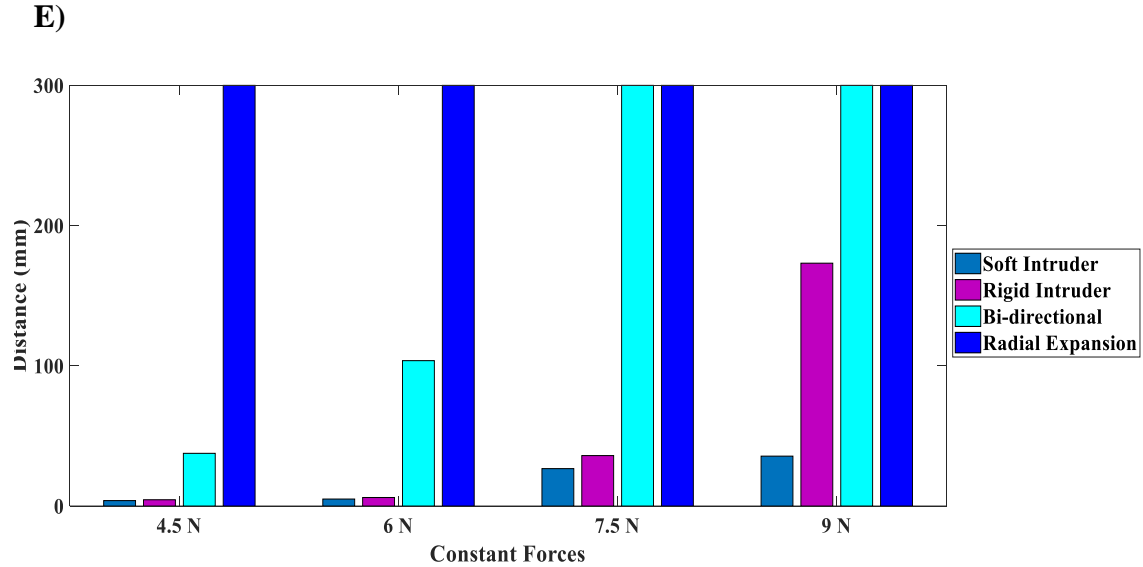


Figure 9 E: Bar graph summarizing distances traveled for all four constant force cases for the different soft-robot segment configurations.

3.2 Constant Velocity Single-Segment Experiments

The results of the constant velocity experiments are summarized in Fig. 10D. The robot segment configuration of periodic radial expansion experienced the lowest drag force for all three cases of constant velocity (0.5 mm/sec, 1 mm/sec, and 2 mm/sec, Fig. 10A-C). The rigid intruder experienced the second lowest drag force, and the intruder that experienced the most drag force was the soft unactuated intruder. The bi-directional bending configuration experienced slightly more drag force than the rigid robot segment configuration. Lastly, to get an idea of the drag force that the system was experiencing without intruders attached, we ran the same tests to get a baseline of drag. The baseline

was consistent and less than the drag force that periodic radial expansion was experiencing.

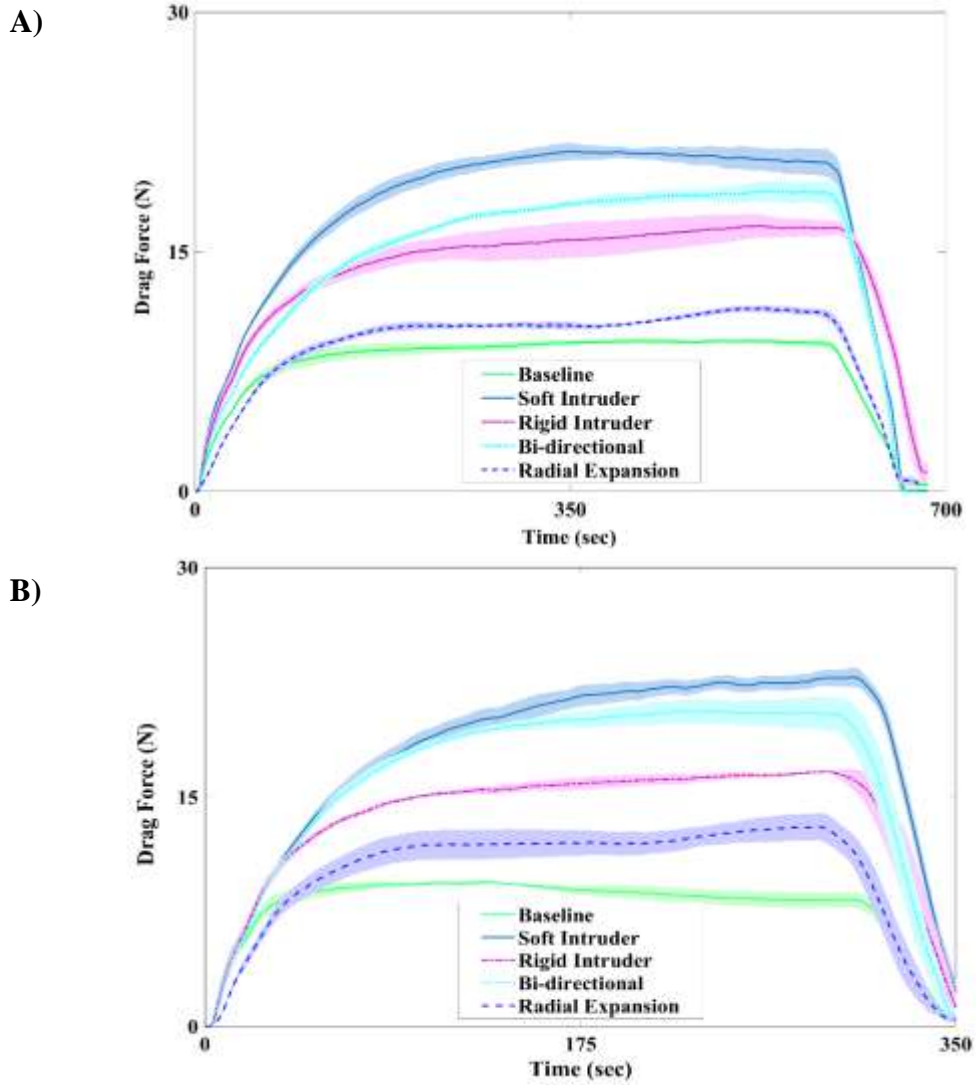


Figure 10 A-B: Results of constant velocity experiments where deflection of the aluminum drag arm was measured. (A)-(B) Raw data of the constant velocity experiments: 0.5 mm/sec (A) and 1 mm/sec (B). The shaded region of the raw data graphs represents the standard error.

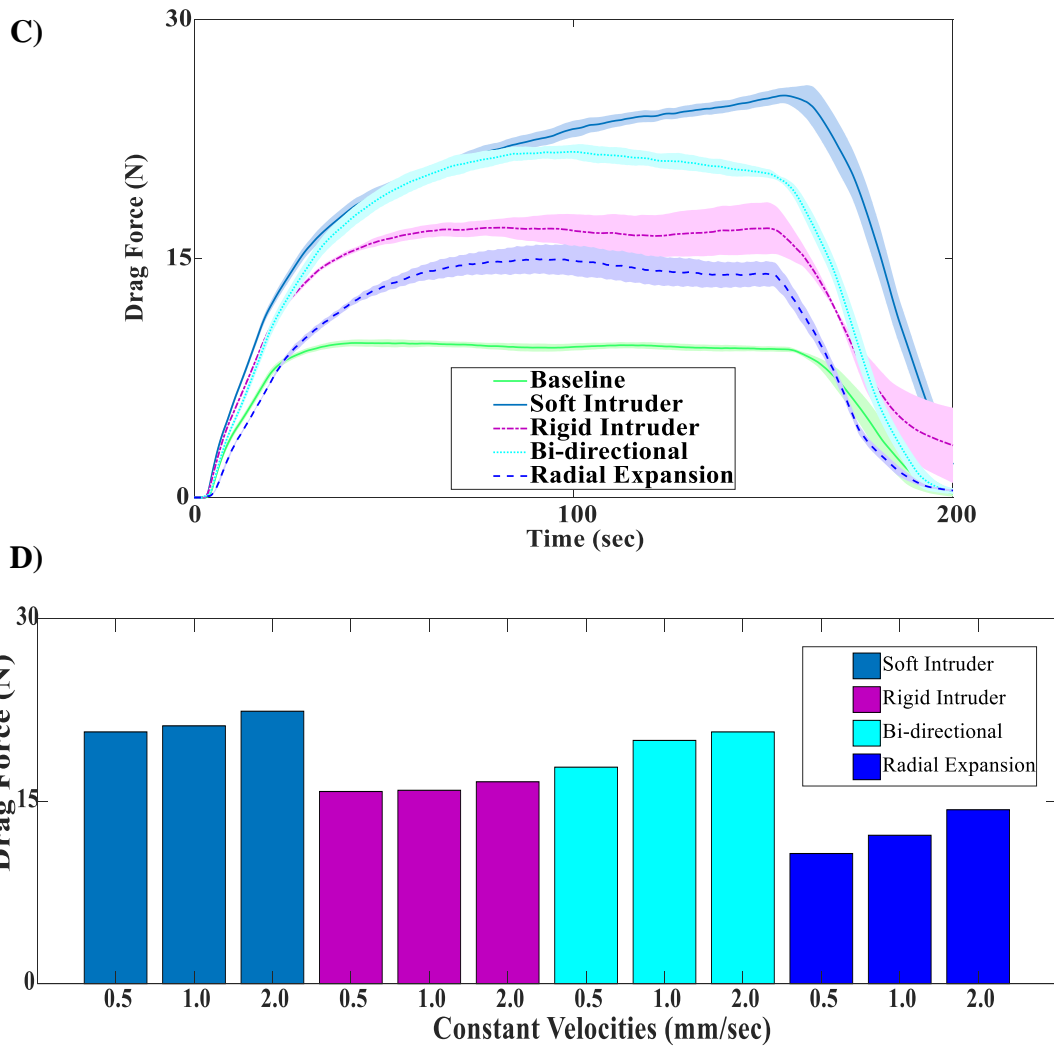


Figure 10 C-D: Results of constant velocity experiments where deflection of the aluminum drag arm was measured. Raw data of the constant velocity experiments at 2.0 mm/sec (C) Summary of Raw data for all velocities (D). The shaded region of the raw data graphs represents the standard error.

3.3 Tethered Three-Segment Digging

The unassisted experiment demonstrated that the three- segment soft-robot could locomote in GS. We observed that the soft system was able to maneuver for some time below the surface of the granular material; however, we witnessed the presence of a lift force. We found that if the system was not submerged below five cm it would eventually follow the path of least resistance and rise to the surface after approximately 12-15 mins of the experiment. This lift force that we observed was also reported for the simple case of a cylinder traveling through granular media [9].

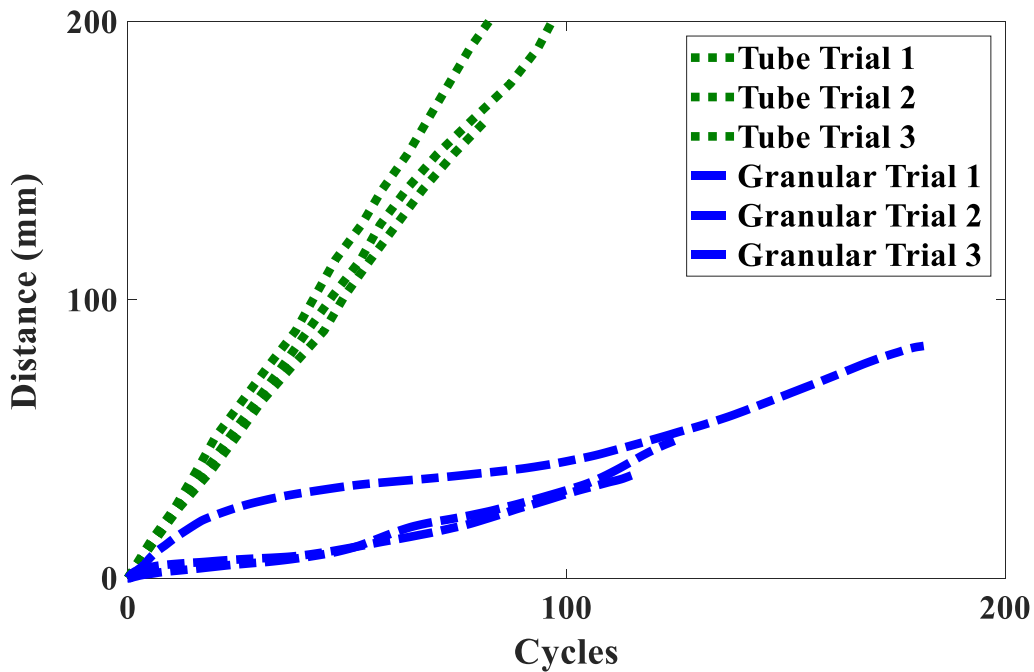


Figure 11: Results of the unassisted experiments both in the granular environment and the acrylic tube for comparison. These experiments were performed three times each.

For these experiments we decided to submerge the system beyond the depth of five cm to approximately eight cm and from this change we were able to gather a longer duration of data while still maintaining locomotion. The unassisted granular experiment resulted in an average velocity of 0.10 mm/sec and maximum distance traveled of 84 mm (Fig. 11). For the case of the structured tube experiment the average velocity of locomotion was 0.54 mm/sec over 150 mm distance of pipe (Fig. 11).

Chapter 4

Discussion

When we compared the velocity measurements of the constant force experiments for the robot segments with no actuation, the rigid intruder was able to travel a much longer distance for all cases of a constant force being applied. The poor performance of the unactuated soft intruder is likely due to the soft intruder's compliance causing it to deform perpendicular to the direction of movement. This deformation likely resulted in an increase in the surface area along the drag direction and thus caused it to experience more drag.

For the comparison of radial expansion and bi-directional bending, we can see that radial expansion outperformed bi-directional bending (Fig. 9). This result from the constant force experiments is likely due to the radial expansion being able to create larger cavitation and disrupt more resistive force chains in the GS. We also observed an acceleration at the beginning of the trials, which is believed to be an initial loosening of the surrounding particles just before data collection was initiated. Despite this observation, the robot segments almost all reached a steady state after approximately 100 mm of travel (except for the unactuated configurations).

Similar to the constant force experiments, in the constant velocity experiments the unactuated soft intruder experienced the most drag at all velocities (Fig. 10D). We also saw that periodic radial expansion or peristaltic motion experienced the least amount of drag force for all the constant velocities tested. Radial expansion likely experienced less drag because it moved a larger volume of particles and thus disrupting more force chains in the granular material. We also observed that bi-directional bending experienced more drag force than the rigid intruder. This behavior is likely due to material filling the cavitation faster than the intruder is moving forward causing the bi-directional bending to experience more drag force.

In comparing the performance of the tethered robot in granular material to the acrylic tube we noticed that the former dug at 18% of the speed of the ideal case. This result highlights both the ability of the soft robot to dig, and the challenges of locomoting in granular substrates. We did not test the limits of depth at which the system would be capable of locomoting below the surface, and it is still unknown how much depth affects the soft robot's ability to move.

Chapter 5

Conclusion

This paper studies how actuation strategies of a soft robot can reduce drag force during locomotion within granular environments. The actuation strategies in this study are inspired by the soft-bristle worm (*polychaeta*). The results of our work demonstrate that a tethered soft robotic system is capable of locomotion in GS despite (and indeed enabled by) a lack of rigid components. We also show that behaviors observed in the soft bristle worm (*polychaeta*), specifically peristaltic expansion, can help reduce drag forces associated with locomotion in GS. This study gives insight that could potentially help in the design of future digging robots for applications such as construction, pipe inspection, exploration of hazardous environments, and subsurface exploration on other planets. Future work could investigate untethering the soft robotic system, the addition of sensors for feedback, and gait sequence optimization. Overall the results presented here form the basis for describing the principles of soft robotic interaction in granular substrates.

I would like to acknowledge Professor Michael Tolley and Professor Nicholas Gravish for coauthoring this thesis in full, which has been submitted for publication as it may appear in IEEE Xplore, 2019, Ortiz, Daniel; Gravish, Nick; and Tolley, T. Michael. The thesis author was the primary investigator and author of this material.

References

- [1] R. Albert, M. A. Pfeifer, A. Barabási, and P. Schiffer, “Slow Drag in a Granular Medium,” *Phys. Rev. Lett.*, pp. 205–208, 1999.
- [2] N. Gravish, P. B. Umbanhowar, and D. I. Goldman, “Force and flow transition in plowed granular media,” *Phys. Rev. Lett.*, vol. 105, no. 12, pp. 1–4, 2010.
- [3] A. A. Zaidi and C. Müller, “Vertical drag force acting on intruders of different shapes in granular media,” vol. 02011, pp. 2–5, 2017.
- [4] P. B. Umbanhowar, N. Gravish, and D. I. Goldman, “Impact, Drag, and the Granular Critical State,” pp. 4–5, 2012.
- [5] G. Hill, S. Yeung, and S. A. Koehler, “Scaling vertical drag forces in granular media,” *Europhys. Lett.*, vol. 72, no. 1, pp. 137–143, 2005.
- [6] N. a. Frigerio and M. J. Shaw, “a Simple Method for Determination of Glutaraldehyde,” *J. Histochem. Cytochem.*, vol. 17, no. 3, pp. 176–181, 1969.
- [7] N. Gravish, P. B. Umbanhowar, and D. I. Goldman, “Force and flow at the onset of drag in plowed granular media,” *Phys. Rev. E - Stat. Nonlinear, Soft Matter Phys.*, vol. 89, no. 4, pp. 1–10, 2014.
- [8] F. Guillard, Y. Forterre, and O. Pouliquen, “Origin of a depth-independent drag force induced by stirring in granular media,” *Phys. Rev. E - Stat. Nonlinear, Soft Matter Phys.*, vol. 91, no. 2, pp. 1–6, 2015.
- [9] Y. Ding, N. Gravish, and D. I. Goldman, “Drag induced lift in granular media,” *Phys. Rev. Lett.*, vol. 106, no. 2, pp. 1–4, 2011.
- [10] W. Kang, Y. Feng, C. Liu, and R. Blumenfeld, “Archimedes’ law explains penetration of solids into granular media,” *Nat. Commun.*, vol. 9, no. 1, pp. 1–9, 2018.
- [11] C. Liu, H. Wan, L. Wang, and P. Wu, “Forces on a cylinder intruder associating rotation and plugging/pulling,” *Powder Technol.*, vol. 322, pp. 41–46, 2017.
- [12] C. R. Wassgren, J. A. Cordova, R. Zenit, and A. Karion, “Dilute granular flow around an immersed cylinder,” *Phys. Fluids*, vol. 15, no. 11, pp. 3318–3330, 2003.
- [13] N. D. Naclerio, C. M. Hubicki, Y. O. Aydin, D. I. Goldman, and E. W. Hawkes, “Soft Robotic Burrowing Device with Tip-Extension and Granular Fluidization,” pp. 5918–5923, 2018.
- [14] N. Algarra, P. G. Karagiannopoulos, A. Lazarus, D. Vandembroucq, and E. Kolb, “Bending transition in the penetration of a flexible intruder in a two-dimensional dense granular medium,” *Phys. Rev. E*, vol. 97, no. 2, pp. 1–12, 2018.

- [15] M. S. Verma, A. Ainla, D. Yang, D. Harburg, and G. M. Whitesides, “A Soft Tube-Climbing Robot,” *Soft Robot.*, vol. 5, no. 2, p. soro.2016.0078, 2017.
- [16] A. D. Marchese, C. D. Onal, and D. Rus, “Autonomous Soft Robotic Fish Capable of Escape Maneuvers Using Fluidic Elastomer Actuators,” *Soft Robot.*, vol. 1, no. 1, pp. 75–87, 2014.
- [17] C. Christianson, N. Goldberg, S. Cai, and M. T. Tolley, “Fluid electrodes for submersible robotics based on dielectric elastomer actuators,” p. 101631O, 2017.
- [18] K. Karakasiliotis, R. Thandiackal, K. Melo, T. Horvat, N. K. Mahabadi, S. Tsitkov, J. M. Cabelguen, and A. J. Ijspeert, “From cineradiography to biorobots: An approach for designing robots to emulate and study animal locomotion,” *J. R. Soc. Interface*, vol. 13, no. 119, 2016.
- [19] B. Zhong Y. O. Aydin, C. Gong, G. Sartoretti, Y. Wu, J. Rieser, H. Xing, J. Rankin, K. Michel, A. Nicieza, J. Hutchinson, D. I. Goldman, and H. Choset, “Coordination of back bending and leg movements for quadrupedal locomotion,” *Robot. Sci. Syst.*, 2018.
- [20] H. Marvi, C. Gong, N. Gravish, H. Astley, M. Travers, R. L. Hatton, J. R Mendelson III, H. Choset, D. L. Hu, D. I. Goldman “Sidewinding with minimal slip: Snake and robot ascent of sandy slopes,” *Science (80-.)*, vol. 346, no. 6206, pp. 224–229, 2014.
- [21] A. G. V Winter, R. L. H. Deits, D. S. Dorsch, A. H. Slocum, and A. E. Hosoi, “Razor clam to RoboClam: Burrowing drag reduction mechanisms and their robotic adaptation,” *Bioinspiration and Biomimetics*, vol. 9, no. 3, 2014.
- [22] R. D. Maladen, Y. Ding, P. B. Umbanhowar, and D. I. Goldman, “Undulatory swimming in sand: Experimental and simulation studies of a robotic sandfish,” *Int. J. Rob. Res.*, vol. 30, no. 7, pp. 793–805, 2011.
- [23] F. Qian, T. Zhang, W. Korff, P. B. Umbanhowar, R. J. Full, and D. I. Goldman, “Principles of appendage design in robots and animals determining terradynamic performance on flowable ground,” *Bioinspiration and Biomimetics*, vol. 10, no. 5, p. 56014, 2015.
- [24] A. E. Hosoi and D. I. Goldman, “Beneath Our Feet: Strategies for Locomotion in Granular Media,” *Annu. Rev. Fluid Mech.*, vol. 47, no. 1, pp. 431–453, 2015.
- [25] Y. O. Aydin, B. Chong, C. Gong, J. M. Rieser, J. W. Rankin, K. Michel, A. G. Nicieza, J. Hutchinson, H. Choset, D. I. Goldman, “Geometric Mechanics Applied to Tetrapod Locomotion on Granular Media,” vol. 8064, pp. 595–603, 2013.
- [26] C. Laschi, M. Cianchetti, B. Mazzolai, L. Margheri, M. Follador, and P. Dario, “Soft robot arm inspired by the octopus,” *Adv. Robot.*, vol. 26, no. 7, pp. 709–727, 2012.

- [27] D. Rus and M. T. Tolley, “Design, fabrication and control of soft robots,” *Nature*, vol. 521, no. 7553, pp. 467–475, 2015.
- [28] T. Umedachi and B. A. Trimmer, “Autonomous decentralized control for soft-bodied caterpillar-like modular robot exploiting large and continuum deformation,” *IEEE Int. Conf. Intell. Robot. Syst.*, vol. 2016–Novem, pp. 292–297, 2016.
- [29] K. M. Dorgan, S. R. Arwade, and P. A. Jumars, “Worms as wedges: Effects of sediment mechanics on burrowing behavior,” *J. Mar. Res.*, vol. 66, no. 2, pp. 219–254, 2008.
- [30] J. Che and K. M. Dorgan, “Mechanics and kinematics of backward burrowing by the polychaete *Cirriformia moorei*,” *J. Exp. Biol.*, vol. 213, no. Pt 24, pp. 4272–7, 2010.
- [31] E. A. K. Murphy and K. M. Dorgan, “Burrow extension with a proboscis: mechanics of burrowing by the glycerid *Hemipodus simplex*,” *J. Exp. Biol.*, vol. 214, no. 6, pp. 1017–1027, 2011.
- [32] P. Esselink and L. Zwarts, “Seasonal trend in burrow depth and tidal variation in feeding activity of *Nereis diversicolor*,” *Mar. Ecol. Prog. Ser.*, vol. 56, no. 1985, pp. 243–254, 1989.
- [33] K. M. Dorgan, “Kinematics of burrowing by peristalsis in granular sands,” *J. Exp. Biol.*, vol. 221, no. Pt 10, p. jeb167759, 2018.
- [34] A. A. Calderon, J. C. Ugalde, J. C. Zagal, and N. O. Perez-Arancibia, “Design, fabrication and control of a multi-material-multi-actuator soft robot inspired by burrowing worms,” *2016 IEEE Int. Conf. Robot. Biomimetics, ROBIO 2016*, no. November, pp. 31–38, 2016.
- [35] Y. O. Aydin, J. L. Molnar, D. I. Goldman, and F. L. Hammond, “Design of a soft robophysical earthworm model,” *2018 IEEE Int. Conf. Soft Robot. RoboSoft 2018*, pp. 83–87, 2018.
- [36] S. Seok, C. D. Onal, K. J. Cho, R. J. Wood, D. Rus, and S. Kim, “Meshworm: A peristaltic soft robot with antagonistic nickel titanium coil actuators,” *IEEE/ASME Trans. Mechatronics*, vol. 18, no. 5, pp. 1485–1497, 2013.
- [37] B. Kim, M. G. Lee, Y. P. Lee, Y. Kim, and G. Lee, “An earthworm-like micro robot using shape memory alloy actuator,” *Sensors Actuators, A Phys.*, vol. 125, no. 2, pp. 429–437, 2006.
- [38] L. Xu, H. Chen, J. Zou, W. Dong, G. Gu, L. Zhu, and X. Zhu, “Bio-inspired annelid robot: A dielectric elastomer actuated soft robot,” *Bioinspiration and Biomimetics*, vol. 12, no. 2, 2017.
- [39] T. Nakamura and T. Iwanaga, “Locomotion strategy for a peristaltic crawling robot in a 2-dimensional space,” *Proc. - IEEE Int. Conf. Robot. Autom.*, pp. 238–

- 243, 2008.
- [40] Smooth-On, “Dragon Skin ® 10 NV Technical Bulletin,” 2018.
 - [41] K. C. Galloway, P. Polygerinos, C. J. Walsh, and R. J. Wood, “Mechanically Programmable Bend Radius for Fiber-Reinforced Soft Actuators,” 2013.
 - [42] M. Bobak, P. Polygerinos, C. Keplinger, S. Wennstedt, R. F. Shepherd, U. Gupta, J. Shim, K. Bertoldi, C. J. Walsh, G. M. Whitesides, “Pneumatic Networks for Soft Robotics that Actuate Rapidly The Harvard community has made this article openly available . Please share how this access benefits you . Your story matters .,” 2016.
 - [43] D. P. Holland, E. J. Park, P. Polygerinos, G. J. Bennett, and C. J. Walsh, “The Soft Robotics Toolkit: Shared Resources for Research and Design,” *Soft Robot.*, vol. 1, no. 3, pp. 224–230, 2014.
 - [44] K. Quillin, “Kinematic scaling of locomotion by hydrostatic animals: ontogeny of peristaltic crawling by the earthworm *lumbricus terrestris*,” *J. Exp. Biol.*, vol. 202 (Pt 6), no. 1999, pp. 661–74, 1999.
 - [45] A. Pantet, S. Robert, S. Jarny, and S. Kervella, “Effect of coarse particle volume fraction on the yield stress of muddy sediments from Marennes Oléron Bay,” *Adv. Mater. Sci. Eng.*, vol. 2010, 2010.
 - [46] N. Gravish and D. I. Goldman, “Effect of volume fraction on granular avalanche dynamics,” *Phys. Rev. E - Stat. Nonlinear, Soft Matter Phys.*, vol. 90, no. 3, pp. 1–7, 2014.